

1 **Quantitative reconstruction of early Holocene and last glacial climate on the Balkan**
2 **Peninsula using coupled hydrological and isotope mass balance modelling**

3 Jack H. Lacey ^{a,*} and Matthew D. Jones ^b

4 ^a NERC Isotope Geosciences Facilities, British Geological Survey, Keyworth, Nottingham,
5 UK

6 ^b School of Geography, University of Nottingham, Nottingham, UK

7 * Corresponding author (jackl@bgs.ac.uk)

8 Keywords: Lakes, modelling, stable isotopes, precipitation, water balance, Lake Ohrid

9 **Abstract**

10 We investigate the modern hydrology of Lake Ohrid (Macedonia/Albania) using a combined
11 hydrological and isotope-based modelling approach and present a new evaluation of
12 contemporary water balance and palaeoclimate estimates. The combined model is able to
13 estimate hydrological components that cannot be directly measured, and indicates that
14 sublacustrine spring inflow is in the order of 50% higher than previous estimates and
15 groundwater outflow comprises approximately a third of overall water outflow. In combination
16 with sediment core oxygen isotope data, we used the combined model to quantitatively
17 reconstruct past climate, in particular precipitation, during the early Holocene and last glacial
18 period. Calculated precipitation in the early Holocene was higher than the value for present day
19 and was approximately 44% lower than present during the last glacial, assuming the majority
20 of precipitation fell as snow. The estimated amount of precipitation in the last glacial would
21 have been high enough to provide refugial conditions at Lake Ohrid and to support the
22 continuous existence of arboreal vegetation in the catchment. The improved understanding of
23 the modern isotope hydrology of Lake Ohrid is fundamental for explaining the systematics of

24 past isotope variation and providing context for extended sediment records from the lake,
25 which will provide longer-term palaeoclimate reconstructions covering multiple glacial-
26 interglacial cycles.

27 **1. Introduction**

28 Lake Ohrid, located on the Balkan Peninsula (Figure 1), is thought to be Europe's oldest
29 freshwater lake with continuous lacustrine sedimentation for at least the past 1.2 Ma (Wagner
30 et al., 2017). The sensitivity of Lake Ohrid and its catchment to hydroclimate variability over
31 the last glacial-interglacial cycle has been documented in several studies using the stable
32 isotope composition of carbonates (Leng et al., 2010; Lacey et al., 2015), geochemical and
33 sediment proxies (Vogel et al., 2010; Wagner et al., 2010), and terrestrial vegetation
34 composition from pollen (Wagner et al., 2009; Panagiotopoulos et al., 2013, 2014). In 2013,
35 an International Continental scientific Drilling Program (ICDP) deep drilling campaign, the
36 Scientific Collaboration on Past Speciation Conditions in Lake Ohrid (SCOPSCO) project,
37 recovered a 584-m composite sediment core sequence spanning the entire history of the lake
38 (Wagner et al., 2014, 2017). Analytical work to date encompasses the upper section of this
39 record (ca. <640 ka) and reveals shifts to more positive values in the reconstructed oxygen
40 isotope composition of lake water ($\delta^{18}\text{O}_L$) between glacial and interglacial phases, in particular
41 during the transition between the last glacial and early Holocene (Lacey et al., 2016). This
42 transition from lower glacial to higher interglacial $\delta^{18}\text{O}_L$ is opposite to the trend observed in
43 other lake and speleothem records from the region (e.g. Roberts et al., 2008; Masi et al., 2018).
44 In addition, the pollen record from SCOPSCO cores indicates a good correspondence between
45 changes in the vegetation assemblage and glacial-interglacial cycles, and suggests that moisture
46 availability was an important forcing mechanism in controlling the presence and abundance of
47 arboreal vegetation in the catchment (Sadori et al., 2016).

48 Therefore, to explain the observed changes in $\delta^{18}\text{O}_L$ at Lake Ohrid between glacial and
49 interglacial periods, and to estimate past changes in moisture availability, it is necessary to
50 evaluate the drivers of $\delta^{18}\text{O}$. In the Mediterranean region, water balance is typically considered
51 to be the primary driver of lake stable isotope hydrology (Roberts et al., 2008, 2010), however
52 it is crucial to understand the modern hydrology of individual lake systems to act as a basis for
53 calibrating proxy-based reconstructions of past climate and environmental change.
54 Palaeoclimate investigations based on stable isotope data from Lake Ohrid have so far only
55 utilised simple linear regression models to understand the hydrological balance of the lake. The
56 current understanding of water balance is derived from estimates that have been modelled using
57 a hydrological mass balance approach (Watzin et al., 2002; Matzinger et al., 2006b), which
58 assume negligible groundwater outflow from the lake.

59 In this study, we use existing monitoring datasets to constrain groundwater flows and calculate
60 a new contemporary water balance for Lake Ohrid using coupled hydrological and stable
61 isotope mass balance modelling. We then use this model to provide a quantitative
62 reconstruction of early Holocene and last glacial climate, in particular past changes in
63 precipitation, in order to better explain glacial-interglacial shifts in $\delta^{18}\text{O}_L$ observed in the proxy
64 record (Lacey et al., 2016). The reconstructed changes in climate are also used to test the
65 hypothesis of Sadori et al. (2016) that the Lake Ohrid catchment had sufficient moisture levels
66 during glacial phases to act as a refugium for arboreal vegetation. The new water balance model
67 is critical to providing an improved, quantitative understanding of the modern isotope
68 hydrology of Lake Ohrid, which will be helpful for discerning the systematics of hydroclimate
69 in longer-term reconstructions from Lake Ohrid that cover multiple glacial-interglacial cycles.

70 **2. Study site**

71 Lake Ohrid (693 m a.s.l.; 40°54'-41°10'N, 20°38'-20°48'E; Figure 1) is situated on the border
72 between the Former Yugoslav Republic of Macedonia and Albania in a Pliocene-formed
73 tectonic graben, bounded to the east by the Galičica (2262 m a.s.l.) and Mali Thate (2287 m
74 a.s.l.) mountains and to the west by the Mokra Mountain chain (1500 m a.s.l.). The lake is
75 approximately 30 km long by 15 km wide and covers an area of 358 km². The lake basin has a
76 tub-shaped morphology with a water volume of 50.7 km³, and a maximum and average water
77 depth of 293 m and 150 m, respectively. Lake Ohrid is fed by a direct catchment area of around
78 1000 km², however an underground connection via karst channels to neighbouring Lake Prespa
79 (849 m a.s.l.; 10 km east of Ohrid) expands the watershed to 2600 km² (Amataj et al., 2007).
80 Remaining water input is derived from direct precipitation and river inflow, and output is
81 dominated by evaporation and river outflow. Groundwater outflow is currently assumed to be
82 negligible and has not been observed to date (Wagner et al., 2008).

83 The climate of Lake Ohrid and its watershed is strongly dependent on both Mediterranean and
84 continental influences, owing to the lake's location in a deep valley surrounded by high
85 mountains and its proximity to the Adriatic Sea, and is also modified by the thermal capacity
86 of the lake itself (Watzin et al., 2002). Average monthly air temperatures range between 2°C
87 in winter and 21°C in summer, with absolute minimum and maximum values of approximately
88 -15°C and 40°C in winter and summer, respectively (Figure 2). The annual distribution of
89 precipitation belongs to the Mediterranean pluviometric regime and varies considerably
90 depending on geographical position in the catchment (Watzin et al., 2002). Rainfall stations
91 around the shoreline of Lake Ohrid receive an average precipitation of 773 mm/year (Figure
92 2), however this increases up to 1445 mm/year at higher altitudes in the catchment (Wagner et
93 al., 2008). Prevailing wind directions are governed by the basin morphology, with northerly
94 winds prevailing in winter and southerly winds in summer (Stankovic, 1960; Watzin et al.,
95 2002).

96 **3. Methodology**

97 **3.1 Hydrological mass balance**

98 The annual water mass balance of a well-mixed lake can be described (e.g. Gibson et al., 2002;
99 Steinman et al., 2010) as the change in lake volume (V) per unit time (T), which is a function
100 of the sum of water inputs (I) and outputs (Q), and may be written as

$$101 \quad \frac{dV}{dT} = \sum I - \sum Q \quad (1)$$

102 Water inputs to a lake comprise direct precipitation on the lake surface (P_L), surface runoff (S_i)
103 and groundwater inflow (G_i). Water outputs include evaporation (E), surface outflow (S_q) and
104 groundwater discharge (G_q), such that

$$105 \quad \frac{dV}{dT} = P_L + S_i + G_i - E - S_q - G_q \quad (2)$$

106 For Lake Ohrid, inputs for equation (2) are derived from previous investigations of lake and
107 catchment hydrology as described below.

108 *Precipitation (P_L)*

109 The average annual precipitation recorded at meteorological stations situated throughout the
110 Lake Ohrid catchment varies between 703 and 1445 mm/year, however for stations located
111 close to the lake the yearly average is 773 mm/year (Figure 2; Watzin et al., 2002). Given that
112 Lake Ohrid has a surface area of 358 km², the total amount of precipitation falling over the
113 entire surface area of the lake is calculated to be 8.8 m³/s.

114 *Surface (S_i) and groundwater (G_i) inflow*

115 The primary surface inflow to Lake Ohrid is the River Sateska, which has a total discharge of
116 7.2 m³/s (Figure 2; Watzin et al., 2002). However, as the river was previously a direct tributary

117 of the main outflow from Ohrid and diverted into the lake in 1962, we do not incorporate the
118 Sateska inflow in our calculations here as our focus is on the long-term palaeo record (the
119 impact on the isotope composition of lake water, δ_L , is discussed later). Other tributaries, for
120 example the Pogradec, Koselka, and Verdova rivers, and catchment runoff have lower
121 discharge rates totalling $7.2 \text{ m}^3/\text{s}$ (Watzin et al., 2002).

122 Groundwater inflow to Lake Ohrid occurs through a network of surface and sub-lacustrine
123 springs. The surface springs consist of three main complexes to the south and north-east of the
124 lake, of which the largest is a collection of 15 springs located at the southern site of St Naum
125 with an average discharge of $7.5 \text{ m}^3/\text{s}$ (Figure 2; Popovska and Bonacci, 2007). To the west of
126 St Naum, near the village of Tushemisht, a second zone comprising 80 springs has an annual
127 discharge of $2.5 \text{ m}^3/\text{s}$ and the Biljana springs to the north-east of Lake Ohrid have a discharge
128 of $0.3 \text{ m}^3/\text{s}$ (Watzin et al., 2002).

129 Artificial and environmental tracer experiments have shown that the water in surface springs
130 is not solely derived from atmospheric precipitation in the catchment, as a proportion is
131 transferred from nearby Lake Prespa through underground karst channels (Amataj et al., 2007;
132 Eftimi et al., 2007). Lake Prespa has a higher surface area to volume ratio in comparison to
133 Lake Ohrid and its waters have a more positive average isotope composition (Leng et al., 2010),
134 which imparts a characteristic shift when combined with meteoric water in the underground
135 karst system. Two-component mixing analysis conducted using stable isotope and Cl- data
136 suggests that the ratio of water originating from Lake Prespa, compared to meteoric
137 precipitation, is around 53% at the Tushemisht springs and 42% at St Naum (Table 1; Anovski
138 et al., 1991; Eftimi and Zoto, 1997; Anovski, 2001; Eftimi et al., 2001; Matzinger et al., 2006a).
139 The Biljana spring waters are derived solely from meteoric precipitation and not influenced by
140 Lake Prespa (Eftimi et al., 2007).

141 The surface springs around Lake Ohrid receive approximately 4.5 m³/s of water from Lake
142 Prespa (Table 1), however total water outflow from Lake Prespa draining into the underground
143 karst system is estimated to total 7.7 m³/s (Anovski, 2001). The remaining 3.2 m³/s of outflow
144 from Lake Prespa is most likely transferred to Lake Ohrid through the sublacustrine network
145 of springs along the lake's eastern margin (Matzinger et al., 2006a). A precise value for the
146 total inflow derived from the sublacustrine springs is currently unknown. Matzinger et al.
147 (2006b) assume a value of 9.9 m³/s for total sublacustrine spring inflow, thereby implying a
148 meteoric component of 6.7 m³/s when the contribution from Lake Prespa is considered,
149 however this value was determined by closing the balance rather than being a direct measure
150 of flowrate. The meteoric component of sublacustrine spring inflow is therefore unknown and
151 termed G_iX here.

152 *Evaporation (E)*

153 Although a direct measurement of evaporation is unavailable for Lake Ohrid, the rate can be
154 estimated using the Linacre (1992) simplification of the Penman (1948) formula for open water
155 evaporation:

$$156 \quad E = [0.015 + 4 \times 10^{-4} T_a + 10^{-6} z] \times [480(T_a + 0.006 z)/(84 - A) - 40 + 2.3 u (T_a - T_d)] \text{ (mm/day)} \quad (3)$$

158 where T_a is the average air temperature (°C), z is the altitude, A is latitude, u is wind speed
159 (m/s), and T_d is the dew point temperature (T_d = 0.52 T_{min} + 0.60 T_{max} - 0.009 T_{max}² - 2.0 °C).
160 Based on climatological measurements between 1961 and 1990 at Pogradec (Figure 2), the
161 average air temperature at Lake Ohrid is 11.7°C, average maximum temperature is 26.2°C,
162 average minimum temperature is -0.8°C, and average wind speed is 2.3 m/s (Watzin et al.,
163 2002). Using Equation 3 (Linacre, 1992), evaporation from Lake Ohrid is estimated to be 13.7

164 m³/s, which is similar to a previous estimate calculated using Penman (1948) of 13.0 m³/s
165 (Watzin et al., 2002; Matzinger et al., 2006b).

166 *Surface (S_q) and groundwater (G_q) outflow*

167 The only surface outflow from Lake Ohrid is the river Crn Drim at the northern margin of the
168 lake, which has a measured average discharge rate of 22 m³/s (Watzin et al., 2002). When the
169 diversion of the River Sateska is considered, and assuming that any increased outflow is
170 directly proportional to increased inflow, the pre-1962 rate is taken to be 14.8 m³/s.

171 Groundwater outflow from Lake Ohrid has not been observed to date (Wagner et al., 2008) and
172 is not considered by previous water balance models (Watzin et al., 2002; Matzinger et al.,
173 2006b). However, given that Triassic limestone crops out along the western margin of Lake
174 Ohrid and the basin is characterised by active faulting (Reicherter et al., 2011; Lindhorst et al.,
175 2015), the potential for a component of groundwater outflow should not be excluded.

176 *Hydrological mass balance*

177 A revised water balance for Lake Ohrid that includes estimates for groundwater fluxes into and
178 out of the lake, based on data outlined above, is shown in Table 2. The unquantified component
179 of groundwater input through the sublacustrine spring network sourced from meteoric
180 precipitation is substituted as G_iX. If a steady state is assumed for Lake Ohrid, such that no
181 change in lake volume is observed over a given period (dV/dT = 0), then the sum of water
182 inputs is equal to the sum of water outputs and Equation (2) can be rewritten for Lake Ohrid:

$$183 \quad P_L + S_i + G_iP + G_iS + G_iX = E + S_q + G_q \quad (4)$$

184 where G_i comprises the output from Lake Prespa (G_iP), and the measured surface spring (G_iS)
185 and unknown sublacustrine spring (G_iX) components of groundwater inflow derived from
186 meteoric precipitation (i.e. G_i = G_iP + G_iS + G_iX).

187 Using the revised water balance (Table 2) and Equation (4), the hydrological mass balance for
188 Lake Ohrid may be written as

$$189 \quad 29.5 + G_i X = 28.5 + G_q \quad (5)$$

190 which can be simplified to

$$191 \quad G_q - G_i X = 1.0 \text{ (m}^3\text{/s)} \quad (6)$$

192 Although the parameters $G_i X$ and G_q cannot be directly measured, it is possible to calculate
193 their values through isotope mass balance.

194 **3.2 Isotope mass balance**

195 The isotope mass balance of a lake is defined (e.g. Steinman et al., 2010; Gibson et al., 2016;
196 Jones et al., 2016) as the sum of the products of water flux (P_L , S_i , G_i , E , S_q , G_q) and the isotope
197 composition of the respective inflows (δ_{PL} , δ_{Si} , δ_{Gi}) and outflows (δ_E , δ_{Sq} , δ_{Gq}), which can be
198 expressed as

$$199 \quad \frac{dV\delta_L}{dT} = P_L \delta_{PL} + S_i \delta_{Si} + G_i \delta_{Gi} - E \delta_E - S_q \delta_{Sq} - G_q \delta_{Gq} \quad (7)$$

200 *Isotope composition of inflows (δ_{PL} , δ_{Si} , δ_{Gi})*

201 As part of an IAEA Regional Project the isotope composition of precipitation falling directly
202 on the lake's surface (δ_{PL}) was measured at the St Naum spring complex, which determined
203 that mean annual weighted $\delta^{18}\text{O} = -8.4 \text{ ‰}$ and $\delta\text{D} = -52.9 \text{ ‰}$ (Figure 3; Anovski, 2001).

204 We take $\delta^{18}\text{O} = -10.1 \pm 0.5 \text{ ‰}$ and $\delta\text{D} = -67.4 \pm 3.1 \text{ ‰}$, average spring water values from data
205 collected periodically over a 30-year period (Figure 3; Anovski et al., 1980, 1991, 2001; Eftimi
206 and Zoto, 1997; Leng et al., 2010), to represent the isotope composition of surface and
207 groundwater inflows fed directly by atmospheric precipitation (δ_{IN}), such that $\delta_{IN} = \delta_{Si} = \delta_{Gi}$.

208 These values are more negative than for δ_{PL} as infiltration will be principally derived from
 209 precipitation at higher altitudes in the Ohrid catchment (Anovski, 2001), which rises to
 210 approximately 1600 m above lake level in the Galičica mountain range separating Lake Ohrid
 211 and Lake Prespa (Francke et al., 2016). In addition, a large proportion of the precipitation
 212 across the catchment likely falls as snow. The pattern of annual discharge of the River Sateska
 213 is at a maximum in early spring following snowmelt (Figure 2; Matzinger et al., 2006b). Snow
 214 is typically characterised as having a lower isotope composition than the equivalent rainfall as
 215 it reflects fractionation at lower temperatures at within-cloud conditions (Gat, 1996; Darling et
 216 al., 2006; Dean et al., 2013).

217 The Prespa-fed component of surface and sublacustrine springs is assumed to be homogenous
 218 with Prespa lakewater (δ_{LP}), which has been measured over a 30-year period to have average
 219 $\delta^{18}O = -1.5 \pm 0.6 \text{ ‰}$ and $\delta D = -20.5 \pm 3.6 \text{ ‰}$ (Figure 3; Leng et al., 2010).

220 *Isotope composition of outflows (δ_E , δ_{Sq} , δ_{Gq})*

221 The isotope composition of evaporation (δ_E) is difficult to measure directly, and so is typically
 222 calculated using the Craig and Gordon (1965) evaporation model (e.g. Steinman et al., 2010):

$$223 \quad \delta_E = \frac{(\alpha^* \times \delta_L) - (h \times \delta_A) - \epsilon}{1 - h + (0.001 \times \epsilon_K)} \quad (8)$$

224 where α^* is the reciprocal of the equilibrium isotope fractionation factor (α) calculated for $\delta^{18}O$
 225 (eq. 9) and δD (eq. 10) using the equations of Horita and Wesolowski (1994), and T_w is the
 226 temperature of lake surface water (in degrees K) assumed to be 287.2 K (Stankovic, 1960).

$$227 \quad \ln \alpha = 0.35041 \left(\frac{10^6}{T_w^3} \right) - 1.6664 \left(\frac{10^3}{T_w^2} \right) + 6.7123 \left(\frac{1}{T_w} \right) - 7.685 \times 10^{-3} \quad (9)$$

$$228 \quad \ln \alpha = 1.1588 \left(\frac{T_w^3}{10^9} \right) - 1.6201 \left(\frac{T_w^2}{10^6} \right) + 0.79484 \left(\frac{T_w}{10^3} \right) + 2.9992 \left(\frac{10^6}{T_w^3} \right) - 161.04 \times 10^{-3} \quad (10)$$

229 The normalised relative humidity (h ; eq. 11) is the quotient of the saturation vapour pressure
 230 of the overlying air (e_{s-a}) and the saturation vapour pressure at the surface water temperature
 231 (e_{s-w}) (eq. 12; Steinman et al., 2010), which relates measured relative humidity (RH = 72.0%)
 232 to average annual temperature (T) of air (11.7°C) or lake water (14.0°C).

$$233 \quad h = RH \times \frac{e_{s-a}}{e_{s-w}} \quad (11)$$

$$234 \quad e_{s-a} \text{ \& } e_{s-w} = 6.108 \times e^{\frac{17.27 \times T}{T+237.7}} \quad (12)$$

235 The isotope composition of atmospheric moisture (δ_A) is assumed to be in equilibrium with
 236 precipitation (eq. 13). The equilibrium isotopic separation factor (ε^* ; eq. 14) is the difference
 237 between the isotope composition of precipitation and atmospheric moisture (Gibson et al.,
 238 2002), which is known to be a function of temperature (eq. 9 and 10; Gonfiantini, 1986).

$$239 \quad \delta_A = \delta_P - \varepsilon^* \quad (13)$$

$$240 \quad \varepsilon^* = 1000 \times (1 - \alpha^*) \quad (14)$$

241 In addition to ε^* , the total isotope separation factor (ε ; eq. 15) also comprises a kinetic
 242 component (ε_K ; Gibson et al., 2002), which is constrained for both oxygen and hydrogen (eq.
 243 16 and 17; Gonfiantini, 1986).

$$244 \quad \varepsilon = \varepsilon^* + \varepsilon_K \quad (15)$$

$$245 \quad \varepsilon_K = 14.2 \times (1 - h) \text{ for } \delta^{18}\text{O} \quad (16)$$

$$246 \quad \varepsilon_K = 12.5 \times (1 - h) \text{ for } \delta\text{D} \quad (17)$$

247 In larger lakes, such as Ohrid, evaporation can have a significant influence on the overlying
 248 atmosphere producing a moisture feedback, and it is therefore important to consider the effects
 249 on kinetic fractionation (eq. 18). As lakewater evaporates, the fraction (f) of evaporate

250 incorporated in the overlying atmosphere modifies δ_A by the addition of δ_E to form δ'_A (Gibson
251 et al., 2016).

$$252 \quad \delta'_A = (1 - f)\delta_A + f\delta_E \quad (18)$$

253 In a feedback system, the modified isotope composition of evaporation (δ'_E) is therefore defined
254 as:

$$255 \quad \delta'_E = \frac{(\alpha^* \times \delta_L) - (h \times \delta'_A) - \varepsilon}{1 - h + (0.001 \times \varepsilon_K)} \quad (19)$$

256 In addition to evaporation, outflow through the river Crn Drim (δ_{sq}) and any groundwater flux
257 (δ_{Gq}) is assumed to have the same isotope composition as average δ_L , where $\delta^{18}O = -3.5 \pm 0.3$
258 ‰ and $\delta D = -31.7 \pm 1.6$ ‰ (Figure 3; Anovski et al., 1980, 1991; Eftimi and Zoto, 1997;
259 Matzinger et al., 2006b; Leng et al., 2010).

260 *Isotope mass balance*

261 The revised water balance (Table 2) allows Equation (7) to be re-expressed for Lake Ohrid:

$$262 \quad \frac{dV\delta_L}{dT} = P_L\delta_{PL} + S_i\delta_{IN} + G_iP\delta_{LP} + G_iS\delta_{IN} + G_iX\delta_{IN} - E\delta_{E'} - S_q\delta_L - G_q\delta_L \quad (20)$$

263 Assuming lake volume is constant through time, such that $dV\delta_L/dT = 0$, Equation (20) can be
264 re-expressed and simplified to

$$265 \quad P_L\delta_{PL} + (S_i + G_iS + G_iX)\delta_{IN} + G_iP\delta_{LP} = E\delta_{E'} + (S_q + G_q)\delta_L \quad (21)$$

266 Given the above, by then iteratively solving equations 18 and 19, for both $\delta^{18}O$ and δD with
267 varying f , and by simultaneously evaluating equations 6 and 21 until G_iX and G_q converge, for
268 both $\delta^{18}O$ and δD scenarios, a balanced model, both hydrologically and isotopically, for Lake
269 Ohrid can be obtained.

270 **4. Results and discussion**

271 **4.1. Isotope mass balance**

272 The iterative calculation of G_iX and G_q suggests flow rates of 15.3 and 16.3 m³/s, respectively,
273 providing a new estimate of water balance for Lake Ohrid (Table 3). Sublacustrine spring
274 inflow of 15.3 m³/s is approximately 50% higher than in existing hydrological models for the
275 lake (e.g. Matzinger et al., 2006b), and groundwater outflow, previously assumed to be
276 negligible, of 16.3 m³/s comprises roughly a third of total water output from Lake Ohrid. For
277 conservation of isotope mass balance the fraction of evaporate incorporated into the overlying
278 atmosphere is approximately $f = 33\%$ (Figure 4), which is of a consistent order of magnitude
279 with other larger lakes such as Lake Superior (40%), Lake Michigan (33%), and Lake Ontario
280 (27%) (Jasechko et al., 2014). The new water balance gives total water output (evaporation,
281 surface and groundwater outflow; Table 3) from Lake Ohrid to be 44.8 m³/s, which, combined
282 with the lake's volume (50.7 km³), suggests a calculated water residence time for the lake of
283 approximately 36 years. As the entire water column experiences complete overturn once every
284 7 years and the upper 200-m on an annual basis (Matzinger et al., 2006b, 2007), the lake water
285 mixes completely several times within the calculated residence time, which may be lower than
286 actual residence time by up to a factor of 4 (Ambrosetti et al., 2003; Wagner et al., 2017).
287 Further, the new calculated value for total water input is < 3% of the overall lakewater volume,
288 and given the lake is well-mixed within its water residence time, any seasonal and inter-annual
289 variations in δ_L will likely be buffered by the large volume and long residence time. This is
290 highlighted by the contemporary monitoring data (Figure 3), which show that δ_L has remained
291 very consistent over the past 30 years and that the lake is an isotopically well-mixed system
292 ($\delta^{18}O = -3.5 \pm 0.3 \text{ ‰}$; Leng et al., 2013 and references therein).

293 **4.2 Estimating past hydrological balance**

294 Isotope-based reconstructions of past climate require a good understanding of the
295 contemporary hydrological system, and by using the established stable isotope mass balance
296 model for the modern environment (as presented above) we can use isotope measurements
297 from core sequences to give quantitative estimates of past changes in the hydrological balance
298 at Lake Ohrid. Over the past 640 ka, one of the largest changes in reconstructed $\delta^{18}\text{O}_L$ is
299 between the last glacial and the Holocene (Lacey et al., 2016). Average $\delta^{18}\text{O}_L$ during the last
300 glacial is roughly 3 ‰ more negative than during the Holocene (Lacey et al., 2016), which is
301 the same magnitude of change as indicated for neighbouring Lake Prespa (Leng et al., 2013).
302 This substantial shift in $\delta^{18}\text{O}_L$ could be related to changes in moisture availability, which is
303 also suggested to be a primary driver of changes in catchment vegetation (Lézine et al., 2010;
304 Panagiotopoulos et al., 2014; Sadori et al., 2016). Moisture availability is important for
305 sustaining tree populations and it has been suggested that the Lake Ohrid catchment received
306 enough moisture to enable the survival of arboreal vegetation, even during glacial periods
307 (Sadori et al., 2016). However, glacial phases are typically characterised by more positive $\delta^{18}\text{O}$
308 values in central and eastern Mediterranean lake sequences (Roberts et al., 2008; Giaccio et al.,
309 2015) and in speleothem records (Regattieri et al., 2018).

310 To better qualify the extent of water availability, and the precipitation changes that control it,
311 across this time frame, we reconstruct here the change in precipitation during the last glacial
312 and the early Holocene using the stable isotope mass balance model for Lake Ohrid and
313 compare the output to other regional records and climate models.

314 *Precipitation (P_L), surface inflows (S_i) and groundwater inflow (G_i)*

315 Values for P_L at Lake Ohrid during the early Holocene and last glacial are unknown. The
316 inflows S_i , G_iS , and G_iX are all a component of catchment-derived meteoric precipitation,
317 therefore the values can be represented by a single inflow term, I_i , where:

318 $I_i = S_i + G_i S + G_i X$ (22)

319 If precipitation over the catchment increases or decreases, P_L will change together with
320 concomitant change in the components of I_i . For estimating past hydrological balance, we
321 assume that variations in P_L and I_i during the early Holocene and last glacial are consistent with
322 their present-day ratio. As P_L is equivalent to $8.8 \text{ m}^3/\text{s}$ and I_i to $27.8 \text{ m}^3/\text{s}$ (Table 3; Equation
323 22), then:

324 $I_i = 3.2 \times P_L$ (23)

325 We take the present outflow from Lake Prespa ($G_i P$) to be constant for the early Holocene and
326 last glacial at $7.7 \text{ m}^3/\text{s}$.

327 *Evaporation (E), surface outflow (S_q), and groundwater outflow (G_q)*

328 To estimate past rates of evaporation, a pollen record from nearby Lake Maliq can be used to
329 evaluate local temperature change. The average temperature difference between the present
330 and early Holocene is reconstructed to be -1°C and for the last glacial -7°C (Bordon et al.,
331 2009), which is consistent with the reconstructed pattern of regional temperature change (Davis
332 et al., 2003), also from pollen data. Although there is no way to calculate palaeo-wind speeds,
333 Jones et al. (2007) suggest Late Glacial average wind velocities may be double that of
334 contemporary measured values in the eastern Mediterranean. At Lake Ohrid, maxima in Cr/Ti
335 and Zr/Ti infer stronger wind activity during glacial periods (Vogel et al., 2010), and so a value
336 of 4.6 m/s is used for last glacial wind speed. If it is assumed that maximum and minimum
337 temperatures are similarly reduced as for average temperature, evaporation decreases to 12.3
338 m^3/s during the early Holocene and to $6.3 \text{ m}^3/\text{s}$ in the last glacial.

339 Surface and groundwater outflow for the early Holocene and last glacial are unknown, but as
340 both are a function of lakewater export (Q_q), the parameters S_q and G_q can be combined:

341 $Q_q = S_q + G_q$ (24)

342 *Isotope composition of inflows (δ_{PL} , δ_{IN} , δ_{LP})*

343 In the Mediterranean region, contemporary rainfall isotope data show a positive correlation
344 between temperature and the isotope composition of precipitation (δ_P) of around +0.3 ‰/°C,
345 which compares well with simulated palaeo relationships at the Last Glacial Maximum (LGM;
346 Bard et al., 2002; Zanchetta et al., 2007). There is also a correspondence between the amount
347 of precipitation and δ_P , where modern $\delta^{18}O_P$ decreases by -1.6 ‰ for every 100 mm increase
348 in monthly precipitation (Bard et al., 2002), however as changes in P_L are unknown the amount
349 effect is discussed later. Given the temperature reconstruction from nearby Lake Maliq (Bordon
350 et al., 2009), this implies that δ_P would have been -2.1 ‰ lower in the last glacial (-7 °C) when
351 compared to the late Holocene. When considering glacial-interglacial shifts in δ_P , changes at
352 the source of δ_P must also be taken in to account. Glacial seawater was roughly 1 ‰ higher on
353 average during the LGM due to the expansion of global ice volume (Schrag et al., 2002), and
354 local evaporative enrichment in the Mediterranean resulted in a change of +1.2 ‰ (Paul et al.,
355 2001). In the Ionian Sea, west of Lake Ohrid, the glacial-interglacial change in $\delta^{18}O$ is
356 estimated to be nearer to +1.3 ‰ (Emeis et al., 2000). This suggests that the combined effect
357 of temperature and source $\delta^{18}O$ changes between the last glacial and late Holocene would
358 therefore be approximately -0.8 ‰. Assuming that $\delta^{18}O$ of Mediterranean seawater in the
359 Holocene had a relatively similar isotope composition to today, as observed for the Ionian Sea
360 (Emeis et al., 2000), we take early Holocene (-1 °C) δ_P to be -0.3 ‰ compared to late Holocene
361 values.

362 As temperatures in the early Holocene were similar to those at present, we assume a comparable
363 precipitation regime (rainfall vs. snowfall) and take the variation in δ_P of -0.3 ‰ to also apply
364 for δ_{IN} . However, in the last glacial, much of the precipitation at higher altitudes across the

365 Ohrid-Prespa catchment may have fallen as snow, as indicated by climate model simulations
366 for the region at the Last Glacial Maximum (Robinson et al., 2006). The snow may have also
367 been incorporated into ice sheets during phases of glacial expansion (Ribolini et al., 2011).
368 Snowfall reflects equilibrium conditions at the point of in-cloud formation and so comprises
369 significantly lower $\delta^{18}\text{O}$ (Darling et al., 2006), which is highlighted by Dean et al. (2013) who
370 report snowfall $\delta^{18}\text{O}$ of around -16‰ in the catchment of Lake Nar in central Turkey,
371 compared to typical average rainfall values of around -10.6‰ (Jones et al., 2005). As much
372 of the present stream and spring inflow to Lake Ohrid is fed by higher altitude precipitation
373 over the catchment and spring snowmelt (Matzinger et al., 2006b), we approximate δ_{IN} during
374 the last glacial to $\delta^{18}\text{O} = -16\text{‰}$.

375 The transfer of water from Lake Prespa to Lake Ohrid during the early Holocene and last glacial
376 is assumed constant, although δ_{LP} will vary between the two intervals. Measured $\delta^{18}\text{O}$ for
377 endogenic calcite (Holocene) and authigenic siderite (last glacial) is available from cores
378 recovered from Lake Prespa (core Co1215; Figure 1), where $\delta^{18}\text{O}_{\text{calcite}}$ in the early Holocene is
379 -2.8‰ and $\delta^{18}\text{O}_{\text{siderite}}$ in the last glacial is -1.4‰ (Figure 5; Leng et al., 2010, 2013). Assuming
380 a temperature of 19°C for summer lakewater at Prespa (time of endogenic calcite precipitation)
381 in the early Holocene and 4.7°C (air temperature) for glacial bottom water (environment of
382 authigenic siderite precipitation), δ_{LP} is calculated to be -2.1‰ for the early Holocene (using
383 Hays and Grossman, 1991) and -5.8‰ during the last glacial (using Zhang et al., 2001).

384 $\delta^2\text{H}$ is estimated for δ_{PL} , δ_{IN} , and δ_{LP} using the modern local evaporation line ($\delta^2\text{H} = 5.4\delta^{18}\text{O} -$
385 12.8), defined by water measurements collated over a ca. 30-year period (Anovski et al., 1980,
386 1991; Eftimi and Zoto, 1997; Anovski, 2001; Matzinger et al., 2006b; Jordanoska et al., 2010;
387 Leng et al., 2010, 2013).

388 *Isotope composition of outflows* (δ_{E} , δ_{Sq} , δ_{Gq})

389 The isotope composition of evaporation is calculated iteratively using equations 18 and 19, and
390 a variable f . This is achieved by simultaneously evaluating hydrological and isotope mass
391 balance equations 25 and 26 to solve for P_L and Q_q (Figure 4), which are balanced for both
392 $\delta^{18}\text{O}$ and δD as in the present-day mass balance model.

$$393 \quad 4.2P_L + G_iP = E + Q_q \quad (25)$$

$$394 \quad P_L\delta_{PL} + 3.2P_L\delta_{IN} + G_iP\delta_{LP} = E\delta_{E'} + Q_q\delta_L \quad (26)$$

395 Equations 25 and 26 are derived by combining equations 4 and 21 with equations 23 and 24,
396 respectively. To calculate δ_E (for use in Equation 18), we take the same temperature change as
397 for calculating E and assume a relative humidity of 73% for the early Holocene (based on the
398 present relationship between RH and temperature) and 50% for the last glacial. Over
399 interglacial-glacial timescales, relative humidity is suggested to reduce with decreasing
400 temperatures as less moisture is available due to lower evaporation rates (Lemcke and Sturm,
401 1997; Jones et al., 2007), and lower RH during the last glacial is confirmed for the Balkan
402 region by a pollen-based humidity-index from the Aegean Sea (Kouli et al., 2012).

403 To determine the past isotope composition of lakewater outflow, assumed to be equivalent to
404 δ_L during respective time periods, we use measured $\delta^{18}\text{O}_{\text{calcite}}$ of -6.0 ‰ for the early Holocene
405 (average for 8.5-9 ka from core Co1262; Lacey et al., 2015) and measured $\delta^{18}\text{O}_{\text{siderite}}$ of -4.0
406 ‰ for the last glacial (average for 16-42 ka from core 5045-1, Figure 5; Lacey et al., 2016). As
407 for the Lake Prespa calculations, we assume a temperature of 19°C for summer lake water in
408 the early Holocene and 4.7°C for glacial bottom water. Conversion to $\delta^{18}\text{O}_L$ gives -5.3 ‰
409 during the early Holocene and -8.1 ‰ during the last glacial (calculated using Hays and
410 Grossman, 1991; Zhang et al., 2001).

411 *Model output and sensitivity tests*

412 The calculated hydrological balance for Lake Ohrid during the early Holocene and last glacial
413 period is given in Table 4. The iterative calculation of P_L suggests that precipitation was around
414 26% higher in the early Holocene ($11.1 \text{ m}^3/\text{s}$ or $978 \text{ mm}/\text{year}$) and 44% lower in the last glacial
415 ($4.9 \text{ m}^3/\text{s}$ or $432 \text{ mm}/\text{year}$), in comparison to the late Holocene (Table 4).

416 The hydrological balance model output is dependent on estimates of past temperature,
417 evaporation, wind speeds, and δ_P (including the isotope composition and seasonality of
418 precipitation). The possible variability in these parameters, and any influence this may have on
419 the calculation of past hydrological balance, can be assessed using sensitivity tests.
420 Palaeotemperatures are estimated from a reconstruction based on a nearby pollen sequence
421 (Bordon et al., 2009), and influence the calculation of evaporative flux from the lake and the
422 amount of direct precipitation (P_L) through the iterative calculation of $\delta'E$. The calculation of
423 past evaporative flux uses estimates for temperature and wind speed, and sensitivity analysis
424 suggests that wind speed has less influence on evaporation compared to changes in temperature
425 (Figure 6). Wind speeds would have to increase to $\sim 22 \text{ m}/\text{s}$ (assuming mean air temperature =
426 $4.7 \text{ }^\circ\text{C}$), or average temperature would have to be similar to the early Holocene ($10.4 \text{ }^\circ\text{C}$;
427 assuming wind speed = $4.6 \text{ m}/\text{s}$), before evaporation during the last glacial was equivalent to
428 the modern evaporative flux. Changing the estimate of past temperature by $\pm 2^\circ\text{C}$ for the
429 iterative calculation of $\delta'E$ and P_L (i.e. twice the reconstructed change between the early and
430 late Holocene; Bordon et al., 2009) suggests that temperature changes do not overly effect the
431 resulting value for P_L , where a $+1^\circ\text{C}$ change leads to $+1 \text{ m}^3/\text{s}$ in P_L in the early Holocene (Table
432 5). This also assumes a simultaneous change in evaporation, with other parameters held
433 constant, as varying air temperature influences the calculation of evaporative flux. In the late
434 Glacial, temperature changes have less effect on P_L than in the early Holocene, as a $+1^\circ\text{C}$
435 change leads to around $+0.7 \text{ m}^3/\text{s}$ in P_L (Table 5).

436 In the last glacial, δ_{IN} is approximated to $\delta^{18}\text{O} = -16 \text{ ‰}$ as high-altitude precipitation in the
437 catchment and snowmelt is a major component of stream and spring inflow to Lake Ohrid, so
438 a greater component of annual precipitation would likely comprise snowfall during colder
439 glacial phases. Sensitivity analysis shows that changes in δ_{IN} only have a minor effect on the
440 calculated value for P_{L} , where varying $\delta^{18}\text{O}_{\text{IN}}$ between -16 ‰ and -13 ‰ produces up to a 2.9
441 m^3/s change in P_{L} (Figure 6). It is only when δ_{IN} approaches δ_{PL} that larger variations in P_{L} are
442 predicted, however δ_{IN} will always be lower than δ_{PL} due to an altitude effect and the elevation
443 difference between Lake Ohrid and its catchment. Therefore, reduced P_{L} during the last glacial
444 is possible even when seasonality changes in precipitation are taken into account.

445 The sensitivity analysis of changing P_{L} with respect to δ_{PL} also suggests that the amount effect,
446 where variable P_{L} forces changes in δ_{PL} , would only drive small changes in calculated values
447 for P_{L} . The relationship between modern monthly precipitation and $\delta^{18}\text{O}$ is around -1.6 ‰ per
448 100 mm change (based on Global Network for Isotopes in Precipitation data from Pisa, Genoa,
449 and Palermo), although this may have been up to -3.9 ‰ per 100 mm at the LGM (Bard et al.,
450 2002). The estimated change in P_{L} in the early Holocene of $+205 \text{ mm/year}$ may therefore equate
451 to an amount effect of between -0.3 ‰ and -3.3 ‰ , depending on the seasonality of additional
452 precipitation. If these values are taken into account and lower δ_{PL} and δ_{IN} are incorporated into
453 the model for the early Holocene the estimated value for P_{L} is reduced, which is unlikely given
454 regional precipitation reconstructions for this time (e.g. Brayshaw et al., 2011; Peyron et al.,
455 2017). Similarly, during the last glacial, the estimated change of -341 mm/year may equate to
456 an amount effect of between $+0.5 \text{ ‰}$ and $+13.3 \text{ ‰}$, depending on the seasonality of
457 precipitation and whether the contemporary or LGM relationship is considered. Sensitivity
458 analysis for the last glacial suggest that varying δ_{PL} results only in a minor change in P_{L} , and
459 only if the seasonality of precipitation was such that δ_{IN} approached δ_{PL} (i.e. restricted snowfall)
460 would changes in δ_{PL} be overly influenced by the amount effect (Figure 6).

461 **4.3 Past hydrological balance**

462 Greater precipitation in the early Holocene is consistent with the shift to lower $\delta^{18}\text{O}$ observed
463 in lake carbonate and speleothem records from across the Balkan Peninsula (Constantin et al.,
464 2007; Francke et al., 2013; Leng et al., 2013; Drăguşin et al., 2014), and a regional shift to
465 lower $\delta^{18}\text{O}$ across other Mediterranean lake records (Lamb et al., 1989; Frogley et al., 2001;
466 Zanchetta et al., 2007; Roberts et al., 2011; Dean et al., 2015). This is further supported by lake
467 level reconstructions from Italy and Greece that indicate deeper water conditions during the
468 early Holocene (Digerfeldt et al., 2000; Magny et al., 2007, 2011; Joannin et al., 2012), and
469 increased river discharge into the Gulf of Salerno (Naimo et al., 2005). Pollen-inferred
470 reconstructions of precipitation from marine and terrestrial records show a wetter regional
471 climate regime across the central and eastern Mediterranean during the early Holocene (Peyron
472 et al., 2017), where rainfall is estimated to have been roughly 20% higher than present in central
473 Anatolia and the southern Levant based on other isotope records (Bar-Matthews et al., 2003;
474 Jones et al., 2007). Global and regional climate model simulations also suggest that the
475 southern Balkan Peninsula experienced one of the largest increases in rainfall during the early
476 Holocene set against stronger precipitation across the Mediterranean region as a whole
477 compared to the present (Brayshaw et al., 2011).

478 The substantial decrease in precipitation calculated for the last glacial period is broadly
479 consistent with pollen-based rainfall estimates for the Late Glacial and Younger Dryas from
480 nearby Lake Maliq (~ 300 mm/year; Bordon et al., 2009), and a 50% reduction in winter
481 precipitation between the Late Glacial and early Holocene over the borderlands of the Aegean
482 Sea (Kotthoff et al., 2008). Model simulations of past climates for the last glacial, typically
483 focussed on the Last Glacial Maximum (ca. 21 ka), indicate reduced precipitation relative to
484 present day, but also suggest that evaporation still likely exceeded precipitation at this time
485 (Robinson et al., 2006), which may be due a southward shift in Mediterranean storm tracks

486 (Goldsmith et al., 2017). The pollen record from Lake Ohrid suggests that glacial periods were
487 typically characterised by cold and dry conditions, as shown by the dominance of non-arboreal
488 pollen indicative of an open environment, which was dominated by steppes and steppe forests
489 during the last two glacial periods (Sadori et al., 2016). However, even during glacial periods,
490 environmental conditions at Lake Ohrid did not appear to cross ecological tolerance thresholds
491 as most arboreal taxa have a continuous presence in the record over the past ca. 500 ka. This
492 suggests that the lake's catchment may have acted as a refugium area for tree populations
493 (Sadori et al., 2016), similar to Lake Ioannina in western Greece (Tzedakis et al., 2002), but in
494 contrast to other eastern Mediterranean sites where arboreal taxa often disappear during
495 glacials due to a more continental climate and lower moisture availability (Okuda et al., 2001;
496 Tzedakis et al., 2004). At Lake Ohrid, the calculated annual precipitation of around 432
497 mm/year (or 4.9 m³/s) during the last glacial (Table 4) is above the threshold of approximately
498 300 mm for the survival of temperate tree populations (e.g. Zohary, 1973). Rainfall is also
499 observed to be greater across the catchment compared to directly over the lake, as average
500 rainfall across the watershed is 907 mm, whereas direct precipitation on the lake is lower at
501 773 mm (Watzin et al., 2002; Popovska and Bonacci, 2007). This suggests that the calculated
502 value for direct precipitation of 432 mm during the last glacial will be lower than for the
503 catchment as a whole. In addition, the fraction of evaporate added to overlying atmospheric
504 vapour is calculated to be only slightly higher than present for the early Holocene (0.36), but
505 is estimated to be much higher for the last glacial (0.73), suggesting that the lake would have
506 provided additional moisture to its surroundings during dry phases. Therefore, the estimate for
507 last glacial precipitation supports the suggestion of Sadori et al. (2016) that refugial conditions
508 most likely occurred in the Lake Ohrid catchment area during glacial periods.

509 **5. Conclusions**

510 This work provides an improved, quantitative understanding of the modern isotope hydrology
511 of Lake Ohrid by re-evaluating groundwater fluxes, which is helpful for explaining the
512 systematics of past climate variations recorded in proxy records from the lake. By incorporating
513 contemporary isotope data into hydrological and isotope mass balance models, we have been
514 able to provide a more robust estimate for the water balance of Lake Ohrid. The new model
515 incorporates underground inflow and outflow components that cannot be directly measured.
516 Groundwater inflow through sublacustrine springs derived from meteoric precipitation is
517 calculated to be 15.3 m³/s, which is around 50% more than predicted in previous water balance
518 models. Groundwater outflow, previously assumed to be negligible, is estimated to be 16.3
519 m³/s and comprise roughly a third of outflow from Lake Ohrid. The new estimate of
520 groundwater outflow decreases the importance of evaporation at only a third of total water
521 output. Therefore, overall changes in the amount of precipitation, and associated changes in
522 throughflow, may have greater influence on $\delta^{18}\text{O}$ rather than isotope variations being
523 intrinsically linked to changes in the precipitation to evaporation ratio.

524 Estimated values for hydrological balance in the early Holocene suggest that precipitation at
525 Lake Ohrid was up to 26% higher than the value for present day, which is consistent with local
526 and regional palaeoclimate records and climate model simulations. Precipitation during the last
527 glacial is calculated to have been around 44% lower than present. The model also suggests that
528 during recent glacial phases the reconstructed shift to low $\delta^{18}\text{O}_L$ from sediment core data can
529 be accounted for, even when precipitation is greatly reduced. This assumes that the majority of
530 precipitation fell in winter as snow within the Lake Ohrid catchment, similar to climate model
531 predictions for the Last Glacial Maximum. The amount of precipitation during the last glacial
532 was above the critical threshold to support the continuous presence of arboreal vegetation
533 within the catchment, suggesting that refugial conditions existed even through glacial phases.

534 **6. Acknowledgements**

535 Part of this work was undertaken during the PhD of JHL which was funded by the British
536 Geological Survey University Funding Initiative (BUFI). We are grateful to Melanie Leng for
537 providing feedback on earlier drafts of this work, and thank Gianni Zanchetta and an
538 anonymous reviewer for their useful comments which significantly improved the final
539 manuscript.

540 **7. References**

541 Amataj, S., Anovski, T., Benischke, R., Eftimi, R., Gourcy, L. L., Kola, L., Leontiadis, I.,
542 Micevski, E., Stamos, A., and Zoto, J., 2007, Tracer methods used to verify the hypothesis of
543 Cvijić about the underground connection between Prespa and Ohrid Lake: *Environmental*
544 *Geology*, v. 51, no. 5, p. 749-753.

545 Ambrosetti, W., Barbanti, L., Sala, N., 2003, Residence time and physical processes in lakes:
546 *Journal of Limnology*, vol. 62, p. 1–15, doi:10.4081/jlimnol.2003.s1.1, 2003.

547 Anovski, T., 2001, Progress in the Study of Prespa Lake Using Nuclear and Related
548 Techniques, IAEA Regional Project RER/8/008, Skopje, Macedonia.

549 Anovski, T., Andonovski, B., and Mineva, B., Study of the hydrological relationship between
550 lakes Ohrid and Prespa, *in* Proceedings Proceedings of an IAEA international symposium,
551 IAEA-SM-Vienna, 11-15 March 1991, Volume 319.

552 Anovski, T., Leontiadis, I., and Zoto, J., 2001, Isotope Data, *in* Anovski, T., ed., Progress in
553 the Study of Prespa Lake Using Nuclear and Related Techniques, IAEA Regional Project
554 RER/8/008: Skopje, Macedonia.

555 Anovski, T., Naumovski, J., Kacurkov, D., and Kirkov, P., 1980, A study of the origin of waters
556 of St. Naum Springs, Lake Ohrid: *Fisika*, v. 12, no. 76-86.

557 Bar-Matthews, M., Ayalon, A., Gilmour, M., Matthews, A., and Hawkesworth, C. J., 2003,
558 Sea-land oxygen isotopic relationships from planktonic foraminifera and speleothems in the
559 Eastern Mediterranean region and their implication for paleorainfall during interglacial
560 intervals: *Geochimica et Cosmochimica Acta*, v. 67, no. 17, p. 3181-3199.

561 Bard, E., Delaygue, G., Rostek, F., Antonioli, F., Silenzi, S., and Schrag, D. P., 2002,
562 Hydrological conditions over the western Mediterranean basin during the deposition of the cold
563 Sapropel 6 (ca. 175 kyr BP): *Earth and Planetary Science Letters*, v. 202, no. 2, p. 481-494.

564 Bordon, A., Peyron, O., Lézine, A.-M., Brewer, S., and Fouache, E., 2009, Pollen-inferred
565 Late-Glacial and Holocene climate in southern Balkans (Lake Maliq): *Quaternary*
566 *International*, v. 200, no. 1-2, p. 19-30.

567 Brayshaw, D. J., Rambeau, C. M. C., and Smith, S. J., 2011, Changes in Mediterranean climate
568 during the Holocene: Insights from global and regional climate modelling: *The Holocene*, v.
569 21, no. 1, p. 15-31.

570 Constantin, S., Bojar, A.-V., Lauritzen, S.-E., and Lundberg, J., 2007, Holocene and Late
571 Pleistocene climate in the sub-Mediterranean continental environment: A speleothem record
572 from Poleva Cave (Southern Carpathians, Romania): *Palaeogeography, Palaeoclimatology,*
573 *Palaeoecology*, v. 243, no. 3-4, p. 322-338.

574 Craig, H., 1961, Isotopic Variations in Meteoric Waters: *Science*, v. 133, p. 1702-1703.

575 Craig, H., and Gordon, L. I., 1965, Deuterium and oxygen 18 variations in the ocean and marine
576 atmosphere, *in* Tongiogi, E., ed., *Stable Isotopes in Oceanographic Studies and*
577 *Paleotemperatures*: Spoleto, Italy, p. 9-130.

578 Darling, W. G., Bath, A. H., Gibson, J. J., and Rozanski, K., 2006, *Isotopes in*
579 *Palaeoenvironmental Research: 1. Isotopes in Water*, Netherlands, Springer.

580 Davis, B. A. S., Brewer, S., Stevenson, A. C., and Guiot, J., 2003, The temperature of Europe
581 during the Holocene reconstructed from pollen data: *Quaternary Science Reviews*, v. 22, no.
582 15-17, p. 1701-1716.

583 Dean, J. R., Jones, M. D., Leng, M. J., Noble, S. R., Metcalfe, S. E., Sloane, H. J., Sahy, D.,
584 Eastwood, W. J., and Roberts, C. N., 2015, Eastern Mediterranean hydroclimate over the late
585 glacial and Holocene, reconstructed from the sediments of Nar lake, central Turkey, using
586 stable isotopes and carbonate mineralogy: *Quaternary Science Reviews*, v. 124, p. 162-174.

587 Dean, J. R., Jones, M. D., Leng, M. J., Sloane, H. J., Roberts, C. N., Woodbridge, J., Swann,
588 G. E. A., Metcalfe, S. E., Eastwood, W. J., and Yiğitbaşıoğlu, H., 2013, Palaeo-seasonality of
589 the last two millennia reconstructed from the oxygen isotope composition of carbonates and
590 diatom silica from Nar Gölü, central Turkey: *Quaternary Science Reviews*, v. 66, p. 35-44.

591 Digerfeldt, G., Olsson, S., and Sandgren, P., 2000, Reconstruction of lake-level changes in lake
592 Xiniás, central Greece, during the last 40 000 years: *Palaeogeography Palaeoclimatology*
593 *Palaeoecology*, v. 158, p. 65-82.

594 Drăguşin, V., Staubwasser, M., Hoffmann, D. L., Ersek, V., Onac, B. P., and Veres, D., 2014,
595 Constraining Holocene hydrological changes in the Carpathian–Balkan region using
596 speleothem $\delta^{18}\text{O}$ and pollen-based temperature reconstructions: *Climate of the*
597 *Past*, v. 10, no. 4, p. 1363-1380.

598 Eftimi, R., Amataj, S., and Zoto, J., 2007, Groundwater circulation in two transboundary
599 carbonate aquifers of Albania; their vulnerability and protection, *in* Witkowski, A. J.,
600 Kowalczyk, A., and Vrba, J., eds., *Groundwater vulnerability assessment and mapping*, Volume
601 11: The Netherlands, Taylor & Francis, p. 206-218.

602 Eftimi, R., Micevski, E., and Stamos, A., 2001, Geological and hydrogeological conditions of
603 the Prespa Region, *in* Anovski, T., ed., Progress in the Study of Prespa Lake Using Nuclear
604 and Related Techniques, IAEA Regional Project RER/8/008: Skopje, Macedonia, p. 11-22.

605 Eftimi, R., and Zoto, J., 1997, Isotope study of the connection of Ohrid and Prespa lakes,
606 International Symposium “Towards Integrated Conservation and Sustainable Development of
607 Transboundary Macro and Micro Prespa Lakes”: Korcha, Albania.

608 Emeis, K. C., Struck, U., Schulz, H. M., Rosenberg, R., Bernasconi, S., Erlenkeuser, H.,
609 Sakamoto, T., and Martinez-Ruiz, F., 2000, Temperature and salinity variations of
610 Mediterranean Sea surface waters over the last 16,000 years from records of planktonic stable
611 oxygen isotopes and alkenone unsaturation ratios: *Palaeogeography Palaeoclimatology*
612 *Palaeoecology*, v. 158, no. 3-4, p. 259-280.

613 Francke, A., Wagner, B., Just, J., Leicher, N., Gromig, R., Baumgarten, H., Vogel, H., Lacey,
614 J. H., Sadori, L., Wonik, T., Leng, M. J., Zanchetta, G., Sulpizio, R., and Giaccio, B., 2016,
615 Sedimentological processes and environmental variability at Lake Ohrid (Macedonia, Albania)
616 between 637 ka and the present: *Biogeosciences*, v. 13, no. 4, p. 1179-1196.

617 Francke, A., Wagner, B., Leng, M. J., and Rethemeyer, J., 2013, A Late Glacial to Holocene
618 record of environmental change from Lake Dojran (Macedonia, Greece): *Climate of the Past*,
619 v. 9, no. 1, p. 481-498.

620 Frogley, M. R., Griffiths, H. I., and Heaton, T. H. E., 2001, Historical biogeography and Late
621 Quaternary environmental change of Lake Pamvotis, Ioannina (north-western Greece):
622 evidence from ostracods: *Journal of Biogeography*, v. 28, no. 6, p. 745-756.

623 Gat, J.R., 1996, Oxygen and hydrogen isotopes in the hydrological cycle: *Annual Review of*
624 *Earth and Planetary Sciences*, v. 24, p. 225-262.

625 Giaccio, B., Regattieri, E., Zanchetta, G., Wagner, B., Galli, P., Mannella, G., Niespolo, E.,
626 Peronace, E., Renne, P.R., Nomade, S., Cavinato, G.P., Messina, P., Sposato, A., Boschi, C.,
627 Florindo, F., Marra, F., and Sadori, L., 2015, A key continental archive for the last 2 Ma of
628 climatic history of the central Mediterranean region: A pilot drilling in the Fucino Basin, central
629 Italy: *Scientific Drilling*, v. 20, p. 13-19.

630 Gibson, J. J., Birks, S. J., and Yi, Y., 2016, Stable isotope mass balance of lakes: a
631 contemporary perspective: *Quaternary Science Reviews*, v. 131, part B, p. 316-328.

632 Gibson, J. J., Prepas, E. E., and McEachern, P., 2002, Quantitative comparison of lake
633 throughflow, residency, and catchment runoff using stable isotopes: modelling and results from
634 a regional survey of Boreal lakes: *Journal of Hydrology*, v. 262, no. 1-4, p. 128-144.

635 Gonfiantini, R., 1986, Environmental isotopes in lake studies. In: Fritz, P., Fontes, J. Ch. (Eds.),
636 *Handbook of Environmental Isotope Geochemistry*, vol. 3, Elsevier, New York.

637 Goldsmith, Y., Polissar, P. J., Ayalon, A., Bar-Matthews, M., deMenocal, P. B., and Broecker,
638 W. S., 2017, The modern and Last Glacial Maximum hydrological cycles of the Eastern
639 Mediterranean and the Levant from a water isotope perspective: *Earth and Planetary Science*
640 *Letters*, v. 457, p. 302-312.

641 Hays, P. D., and Grossman, E. L., 1991, Oxygen isotopes in meteoric calcite cements as
642 indicators of continental paleoclimate: *Geology*, v. 19, p. 441-444.

643 Horita, J., and Wesolowski, D. J., 1994, Liquid-vapor fractionation of oxygen and hydrogen
644 isotopes of water from the freezing to the critical temperature: *Geochimica et Cosmochimica*
645 *Acta*, v. 58, no. 16, p. 3425-3437.

646 Jasechko, S., Gibson, J. J., and Edwards, T. W. D., 2014, Stable isotope mass balance of the
647 Laurentian Great Lakes: *Journal of Great Lakes Research*, v. 40, no. 2, p. 336-346.

648 Joannin, S., Brugiapaglia, E., de Beaulieu, J. L., Bernardo, L., Magny, M., Peyron, O., Goring,
649 S., and Vanni re, B., 2012, Pollen-based reconstruction of Holocene vegetation and climate in
650 southern Italy: the case of Lago Trifoglietti: *Clim. Past*, v. 8, no. 6, p. 1973-1996.

651 Jones, M.D., Leng, M.J., Roberts, C.N., T rkes, M. and Moyeed, R., 2005, A coupled
652 calibration and modelling approach to the understanding of dry-land lake oxygen isotope
653 records: *Journal of Paleolimnology*, v. 34, p. 391-411.

654 Jones, M. D., Roberts, C. N., and Leng, M. J., 2007, Quantifying climatic change through the
655 last glacial–interglacial transition based on lake isotope palaeohydrology from central Turkey:
656 *Quaternary Research*, v. 67, no. 3, p. 463-473.

657 Jones, M.D., Cuthbert, M.O., Leng, M.J., McGowan, S., Mariethoz, G., Arrowsmith, C.,
658 Sloane, H.J., Humphrey, K.K., Cross, I., 2016. Comparisons of observed and modelled lake
659 $\delta^{18}O$ variability. *Quaternary Science Reviews*, v. 131, Part B, p. 329-340.

660 Jordanoska, B., Kunz, M. J., Stafilov, T., and Wuest, A., 2010, Temporal variability in physico-
661 chemical properties of St. Naum karst springs feeding Lake Ohrid: *Ecology and Protection of
662 the Environment*, v. 13, no. 1-2, p. 3-11.

663 Kotthoff, U., Pross, J., M ller, U. C., Peyron, O., Schmiedl, G., Schulz, H., and Bordon, A.,
664 2008, Climate dynamics in the borderlands of the Aegean Sea during formation of sapropel S1
665 deduced from a marine pollen record: *Quaternary Science Reviews*, v. 27, no. 7-8, p. 832-845.

666 Kouli, K., Gogou, A., Bouloubassi, I., Triantaphyllou, M. V., Ioakim, C., Katsouras, G.,
667 Roussakis, G., and Lykousis, V., 2012, Late postglacial paleoenvironmental change in the
668 northeastern Mediterranean region: Combined palynological and molecular biomarker
669 evidence: *Quaternary International*, v. 261, p. 118-127.

670 Lacey, J. H., Francke, A., Leng, M. J., Vane, C. H., and Wagner, B., 2015, A high-resolution
671 Late Glacial to Holocene record of environmental change in the Mediterranean from Lake
672 Ohrid (Macedonia/Albania): *International Journal of Earth Sciences*, v. 104, no. 6, p. 1623-
673 1638.

674 Lacey, J. H., Leng, M. J., Francke, A., Sloane, H. J., Milodowski, A., Vogel, H., Baumgarten,
675 H., Zanchetta, G., and Wagner, B., 2016, Northern Mediterranean climate since the Middle
676 Pleistocene: a 637 ka stable isotope record from Lake Ohrid (Albania/Macedonia):
677 *Biogeosciences*, v. 13, no. 6, p. 1801-1820.

678 Lamb, H. F., Eicher, U., and Switsur, V. R., 1989, An 18 000-year record of vegetation, lake-
679 level and climatic change from Tigalmamine, Middle Atlas, Morocco: *Journal of*
680 *Biogeography*, v. 16, no. 1, p. 65-74.

681 Lemcke, G., and Sturm, M., 1997, $\delta^{18}O$ and Trace Element Measurements as Proxy for the
682 Reconstruction of Climate Changes at Lake Van (Turkey): Preliminary Results, *in* Dalfes, H.
683 N., Kukla, G., and Weiss, H., eds., *Third Millennium BC Climate Change and Old World*
684 *Collapse*: Berlin, Heidelberg, Springer Berlin Heidelberg, p. 653-678.

685 Leng, M. J., Baneschi, I., Zanchetta, G., Jex, C. N., Wagner, B., and Vogel, H., 2010, Late
686 Quaternary palaeoenvironmental reconstruction from Lakes Ohrid and Prespa
687 (Macedonia/Albania border) using stable isotopes: *Biogeosciences*, v. 7, no. 10, p. 3109-3122.

688 Leng, M. J., Wagner, B., Boehm, A., Panagiotopoulos, K., Vane, C. H., Snelling, A., Haidon,
689 C., Woodley, E., Vogel, H., Zanchetta, G., and Baneschi, I., 2013, Understanding past climatic
690 and hydrological variability in the Mediterranean from Lake Prespa sediment isotope and
691 geochemical record over the Last Glacial cycle: *Quaternary Science Reviews*, v. 66, p. 123-
692 136.

693 Lézine, A.-M., von Grafenstein, U., Andersen, N., Belmecheri, S., Ordon, A., Caron, B., Cazet,
694 J.-P., Erlenkeuser, H., Fouache, E., Grenier, C., Huntsman-Mapila, P., Hureau-Mazaudier, D.,
695 Manelli, D., Mazaud, A., Robert, C., Sulpizio, R., Tiercelin, J.-J., Zanchetta, G., and Zeqollari,
696 Z., 2010, Lake Ohrid, Albania, provides an exceptional multi-proxy record of environmental
697 changes during the last glacial–interglacial cycle: *Palaeogeography, Palaeoclimatology,*
698 *Palaeoecology*, v. 287, p. 116–127.

699 Linacre, E., 1992, *Climate Data and Resources: A Reference and Guide*, London, Routledge.

700 Lindhorst, K., Krastel, S., Reicherter, K., Stipp, M., Wagner, B., and Schwenk, T., 2015,
701 *Sedimentary and tectonic evolution of Lake Ohrid (Macedonia/Albania): Basin Research*, v.
702 27, p. 84-101.

703 Magny, M., Bossuet, G., Ruffaldi, P., Leroux, A., and Mouthon, J., 2011, Orbital imprint on
704 Holocene palaeohydrological variations in west-central Europe as reflected by lake-level
705 changes at Cerin (Jura Mountains, eastern France): *Journal of Quaternary Science*, v. 26, no.
706 2, p. 171-177.

707 Magny, M., de Beaulieu, J.-L., Drescher-Schneider, R., Vanni re, B., Walter-Simonnet, A.-V.,
708 Miras, Y., Millet, L., Bossuet, G., Peyron, O., Brugiapaglia, E., and Leroux, A., 2007, Holocene
709 climate changes in the central Mediterranean as recorded by lake-level fluctuations at Lake
710 Accesa (Tuscany, Italy): *Quaternary Science Reviews*, v. 26, no. 13–14, p. 1736-1758.

711 Matzinger, A., Jordanoski, M., Veljanoska-Sarafiloska, E., Sturm, M., M ller, B., and Wuest,
712 A., 2006a, Is Lake Prespa Jeopardizing the Ecosystem of Ancient Lake Ohrid?: *Hydrobiologia*,
713 v. 553, no. 1, p. 89-109.

714 Matzinger, A., Spirkovski, Z., Patceva, S., and Wüest, A., 2006b, Sensitivity of Ancient Lake
715 Ohrid to Local Anthropogenic Impacts and Global Warming: *Journal of Great Lakes Research*,
716 v. 32, no. 1, p. 158-179.

717 Matzinger, A., Schmid, M., Veljanoska-Sarafiloska, E., Patceva, S., Guseska, D., Wagner, B.,
718 Müller, B., Sturm, M., Wüest, A., 2007, Eutrophication of ancient Lake Ohrid: Global warming
719 amplifies detrimental effects of increased nutrient inputs: *Limnology and Oceanography*, v. 52,
720 p. 338-353.

721 Naimo, D., Adamo, P., Imperato, M., and Stanzione, D., 2005, Mineralogy and geochemistry
722 of a marine sequence, Gulf of Salerno, Italy: *Quaternary International*, v. 140-141, p. 53-63.

723 Okuda, M., Yasuda, Y., and Setoguchi, T., 2001, Middle to Late Pleistocene vegetation history
724 and climatic changes at Lake Kopais, Southeast Greece: *Boreas*, v. 30, no. 1, p. 73-82.

725 Outcalt, S.I., Allen, H.L., 1982, Modeling the annual thermal regime of Lake Ohrid,
726 Yugoslavia, using daily weather data: *Ecological Modelling*, v. 15, p. 165-184.

727 Panagiotopoulos, K., Aufgebauer, A., Schäbitz, F., and Wagner, B., 2013, Vegetation and
728 climate history of the Lake Prespa region since the Lateglacial: *Quaternary International*, v.
729 293, p. 157-169.

730 Panagiotopoulos, K., Böhm, A., Leng, M. J., Wagner, B., and Schäbitz, F., 2014, Climate
731 variability over the last 92 ka in SW Balkans from analysis of sediments from Lake Prespa:
732 *Climate of the Past*, v. 10, no. 2, p. 643-660.

733 Paul, H. A., Bernasconi, S. M., Schmid, D. W., and McKenzie, J. A., 2001, Oxygen isotope
734 composition of the Mediterranean Sea since the Last Glacial Maximum: Constraints from pore
735 water analyses: *Earth and Planetary Science Letters*, v. 192, no. 1, p. 1-14.

736 Penman, H. L., 1948, Natural Evaporation from Open Water, Bare Soil and Grass: Proceedings
737 of the Royal Society of London. Series A. Mathematical and Physical Sciences, v. 193, p. 120-
738 145.

739 Peyron, O., Combourieu-Nebout, N., Brayshaw, D., Goring, S., Andrieu-Ponel, V., Desprat,
740 S., Fletcher, W., Gambin, B., Ioakim, C., Joannin, S., Kotthoff, U., Kouli, K., Montade, V.,
741 Pross, J., Sadori, L., and Magny, M., 2017, Precipitation changes in the Mediterranean basin
742 during the Holocene from terrestrial and marine pollen records: a model–data comparison:
743 *Climate of the Past*, v. 13, no. 3, p. 249-265.

744 Popovska, C., and Bonacci, O., 2007, Basic data on the hydrology of Lakes Ohrid and Prespa:
745 *Hydrological Processes*, v. 21, no. 5, p. 658-664.

746 Regattieri, E., Zanchetta, G., Isola, I., Bajo, P., Perchiazzi, N., Drysdale, R.N., Boschi, C.,
747 Hellstrom, J.C., Francke, A., and Wagner, B., 2018, A MIS 9/MIS 8 speleothem record of
748 hydrological variability from Macedonia (F.Y.R.O.M.): *Global and Planetary Change*, v. 162,
749 p. 39-52.

750 Reicherter, K., Hoffmann, N., Lindhorst, K., Krastel, S., Fernández-Steeger, T., Grützner, C.,
751 and Wiatr, T., 2011, Active basins and neotectonics: Morphotectonics of the Lake Ohrid Basin
752 (FYROM and Albania): *Zeitschrift der Deutschen Gesellschaft für Geowissenschaften*, v. 162,
753 no. 2, p. 217-234.

754 Ribolini, A., Isola, I., Zanchetta, G., Bini, M., and Sulpizio, R., 2011, Glacial feature on the
755 Galicica Mountains, Macedonia: preliminary report: *Geografia Fisica e Dinamica Quaternaria*,
756 v. 34, p. 247-255.

757 Roberts, C. N., Zanchetta, G., and Jones, M. D., 2010, Oxygen isotopes as tracers of
758 Mediterranean climate variability: An introduction: *Global and Planetary Change*, v. 71, no. 3-
759 4, p. 135-140.

760 Roberts, N., Brayshaw, D., Kuzucuoglu, C., Perez, R., and Sadori, L., 2011, The mid-Holocene
761 climatic transition in the Mediterranean: Causes and consequences: *The Holocene*, v. 21, no.
762 1, p. 3-13.

763 Roberts, N., Jones, M. D., Benkaddour, A., Eastwood, W. J., Filippi, M. L., Frogley, M. R.,
764 Lamb, H. F., Leng, M. J., Reed, J. M., Stein, M., Stevens, L., Valero-Garcés, B., and Zanchetta,
765 G., 2008, Stable isotope records of Late Quaternary climate and hydrology from Mediterranean
766 lakes: the ISOMED synthesis: *Quaternary Science Reviews*, v. 27, no. 25-26, p. 2426-2441.

767 Robinson, S. A., Black, S., Sellwood, B. W., and Valdes, P. J., 2006, A review of
768 palaeoclimates and palaeoenvironments in the Levant and Eastern Mediterranean from 25,000
769 to 5000 years BP: setting the environmental background for the evolution of human
770 civilisation: *Quaternary Science Reviews*, v. 25, no. 13-14, p. 1517-1541.

771 Sadori, L., Koutsodendris, A., Panagiotopoulos, K., Masi, A., Bertini, A., Combourieu-Nebout,
772 N., Francke, A., Kouli, K., Joannin, S., Mercuri, A. M., Peyron, O., Torri, P., Wagner, B.,
773 Zanchetta, G., Sinopoli, G., and Donders, T. H., 2016, Pollen-based paleoenvironmental and
774 paleoclimatic change at Lake Ohrid (south-eastern Europe) during the past 500 ka:
775 *Biogeosciences*, v. 13, no. 5, p. 1423-1437.

776 Schrag, D. P., Adkins, J. F., McIntyre, K., Alexander, J. L., Hodell, D. A., Charles, C. D., and
777 McManus, J. F., 2002, The oxygen isotopic composition of seawater during the Last Glacial
778 Maximum: *Quaternary Science Reviews*, v. 21, no. 1-3, p. 331-342.

779 Stankovic, S., 1960, *The Balkan Lake Ohrid and Its Living World*, Den Haag, Uitgeverij Dr.
780 W. Junk, *Monographiae Biologicae*.

781 Steinman, B. A., Rosenmeier, M. F., Abbott, M. B., and Bain, D. J., 2010, The isotopic and
782 hydrologic response of small, closed-basin lakes to climate forcing from predictive models:
783 Application to paleoclimate studies in the upper Columbia River basin: *Limnology and*
784 *Oceanography*, v. 55, no. 6, p. 2231-2245.

785 Tzedakis, P. C., Frogley, M. R., Lawson, I. T., Preece, R. C., Cacho, I., and de Abreu, L., 2004,
786 Ecological thresholds and patterns of millennial-scale climate variability: The response of
787 vegetation in Greece during the last glacial period: *Geology*, v. 32, no. 2, p. 109-112.

788 Tzedakis, P. C., Lawson, I. T., Frogley, M. R., Hewitt, G. M., and Preece, R. C., 2002, Buffered
789 tree population changes in a quaternary refugium: evolutionary implications: *Science*, v. 297,
790 no. 5589, p. 2044-2047.

791 Vogel, H., Wagner, B., Zanchetta, G., Sulpizio, R., and Rosén, P., 2010, A paleoclimate record
792 with tephrochronological age control for the last glacial-interglacial cycle from Lake Ohrid,
793 Albania and Macedonia: *Journal of Paleolimnology*, v. 44, no. 1, p. 295-310.

794 Wagner, B., Lotter, A. F., Nowaczyk, N., Reed, J. M., Schwalb, A., Sulpizio, R., Valsecchi,
795 V., Wessels, M., and Zanchetta, G., 2009, A 40,000-year record of environmental change from
796 ancient Lake Ohrid (Albania and Macedonia): *Journal of Paleolimnology*, v. 41, no. 3, p. 407-
797 430.

798 Wagner, B., Reicherter, K., Daut, G., Wessels, M., Matzinger, A., Schwalb, A., Spirkovski, Z.,
799 and Sanxhaku, M., 2008, The potential of Lake Ohrid for long-term palaeoenvironmental
800 reconstructions: *Palaeogeography, Palaeoclimatology, Palaeoecology*, v. 259, no. 2-3, p. 341-
801 356.

802 Wagner, B., Vogel, H., Zanchetta, G., and Sulpizio, R., 2010, Environmental change within
803 the Balkan region during the past ca. 50 ka recorded in the sediments from lakes Prespa and
804 Ohrid: *Biogeosciences*, v. 7, no. 10, p. 3187-3198.

805 Wagner, B., Wilke, T., Francke, A., Albrecht, C., Baumgarten, H., Bertini, A., Combourieu-
806 Nebout, N., Cvetkoska, A., amp, apos, Addabbo, M., Donders, T. H., Föller, K., Giaccio, B.,
807 Grazhdani, A., Hauffe, T., Holtvoeth, J., Joannin, S., Jovanovska, E., Just, J., Kouli, K.,
808 Koutsodendris, A., Krastel, S., Lacey, J. H., Leicher, N., Leng, M. J., Levkov, Z., Lindhorst,
809 K., Masi, A., Mercuri, A. M., Nomade, S., Nowaczyk, N., Panagiotopoulos, K., Peyron, O.,
810 Reed, J. M., Regattieri, E., Sadori, L., Sagnotti, L., Stelbrink, B., Sulpizio, R., Tofilovska, S.,
811 Torri, P., Vogel, H., Wagner, T., Wagner-Cremer, F., Wolff, G. A., Wonik, T., Zanchetta, G.,
812 and Zhang, X. S., 2017, The environmental and evolutionary history of Lake Ohrid
813 (FYROM/Albania): interim results from the SCOPSCO deep drilling project: *Biogeosciences*,
814 v. 14, no. 8, p. 2033-2054.

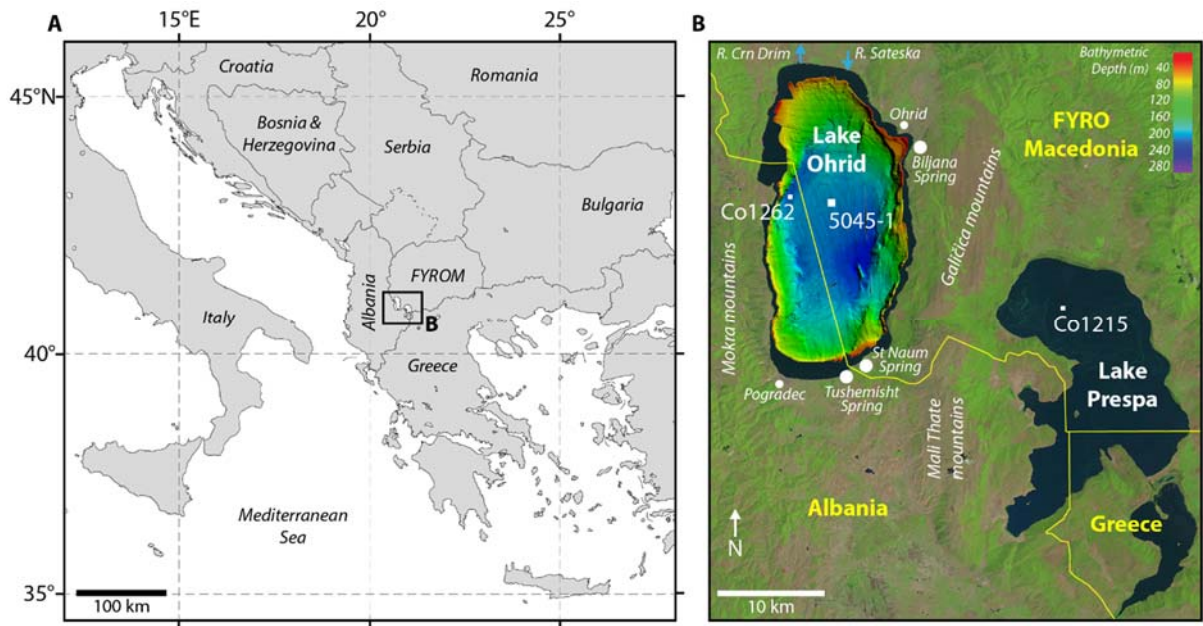
815 Wagner, B., Wilke, T., Krastel, S., Zanchetta, G., Sulpizio, R., Reicherter, K., Leng, M. J.,
816 Grazhdani, A., Trajanovski, S., Francke, A., Lindhorst, K., Levkov, Z., Cvetkoska, A., Reed,
817 J. M., Zhang, X., Lacey, J. H., Wonik, T., Baumgarten, H., and Vogel, H., 2014, The
818 SCOPSCO drilling project recovers more than 1.2 million years of history from Lake Ohrid:
819 *Scientific Drilling*, v. 17, p. 19-29.

820 Watzin, M. C., Puka, V., and Naumoski, T. B., 2002, Lake Ohrid and its watershed, state of
821 the environment report, Macedonia, Tirana, Lake Ohrid Conservation Project.

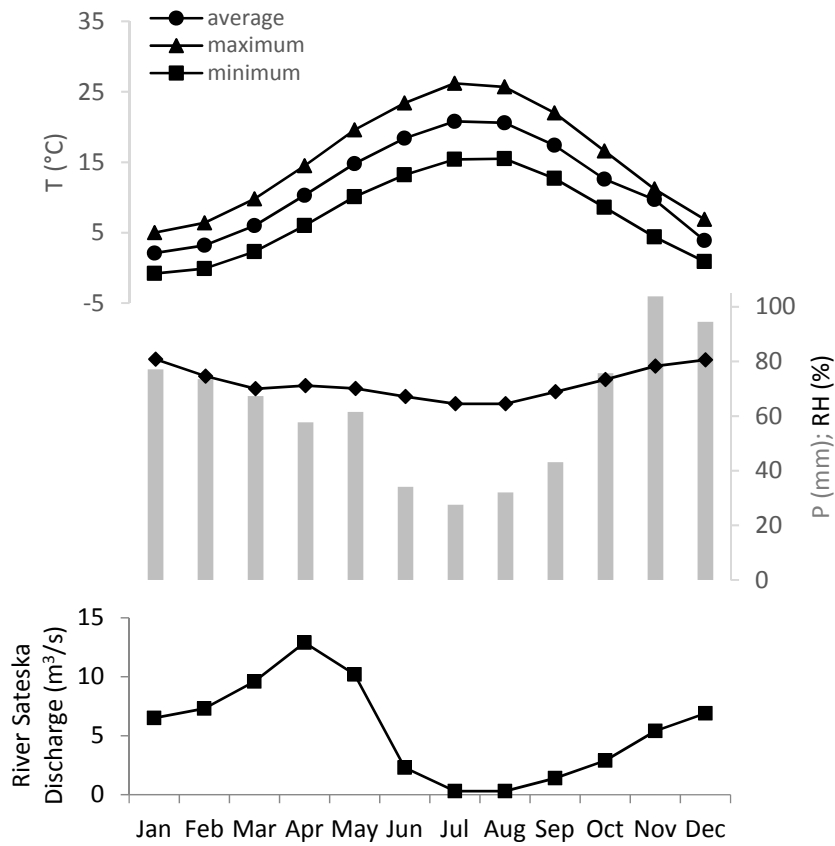
822 Zanchetta, G., Borghini, A., Fallick, A. E., Bonadonna, F. P., and Leone, G., 2007, Late
823 Quaternary palaeohydrology of Lake Pergusa (Sicily, southern Italy) as inferred by stable
824 isotopes of lacustrine carbonates: *Journal of Paleolimnology*, v. 38, no. 2, p. 227-239.

- 825 Zhang, C. L., Horita, J., Cole, D. R., Zhou, J. Z., Lovley, D. R., and Phelps, T. J., 2001,
826 Temperature-dependent oxygen and carbon isotope fractionations of biogenic siderite:
827 *Geochimica et Cosmochimica Acta*, v. 65, no. 14, p. 2257-2271.
- 828 Zohary, M., 1973, *Geobotanical foundations of the Middle East*, Stuttgart, Fischer.

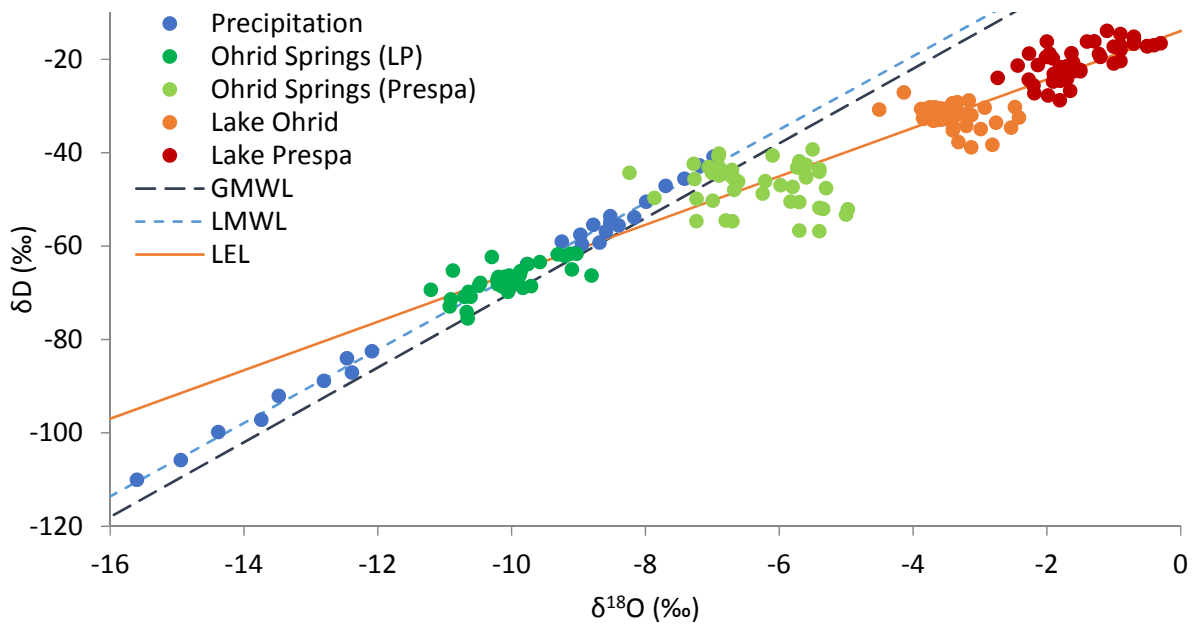
829 **Figure 1** (A) Location of Lake Ohrid and Lake Prespa on the Balkan Peninsula (black
830 rectangle), and (B) map of the Ohrid and Prespa basins, showing bathymetry of Lake Ohrid
831 (Lindhorst et al., 2015). The location of coring sites mentioned in the text (5045-1, Co1262,
832 Co1215; Leng et al., 2013; Lacey et al., 2015, 2016; Wagner et al., 2017) are shown by white
833 squares.



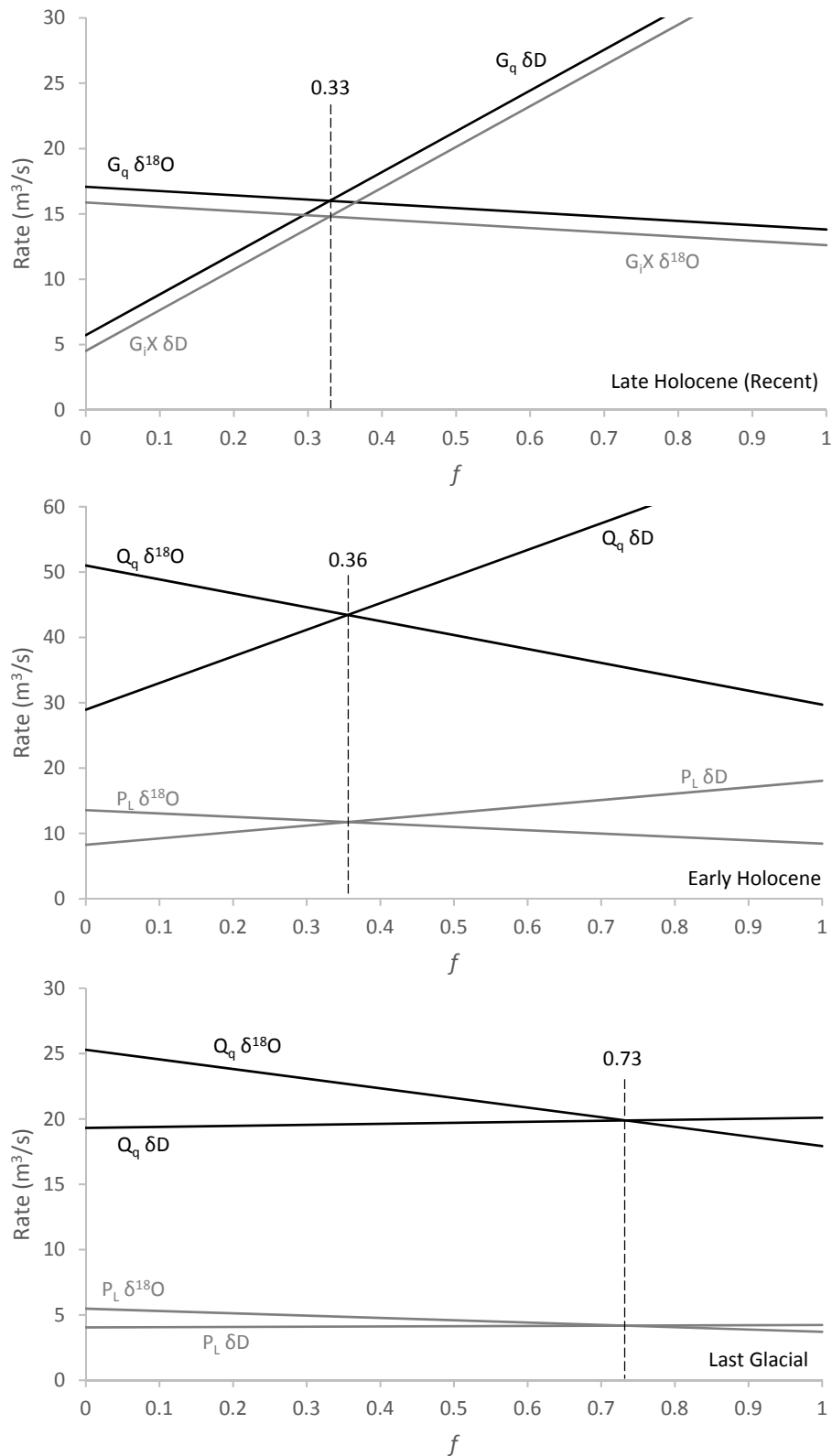
834 **Figure 2** Climatological indices of air temperature (T) and precipitation (P) from the
 835 meteorological station at Pogradec, Albania (1961-1990; Watzin et al., 2002), relative humidity
 836 (RH) from the station at Bitola (1972-1977; Outcalt and Allen, 1982), and the seasonal
 837 discharge of the River Sateska (1996-2000; Matzinger et al., 2006b).



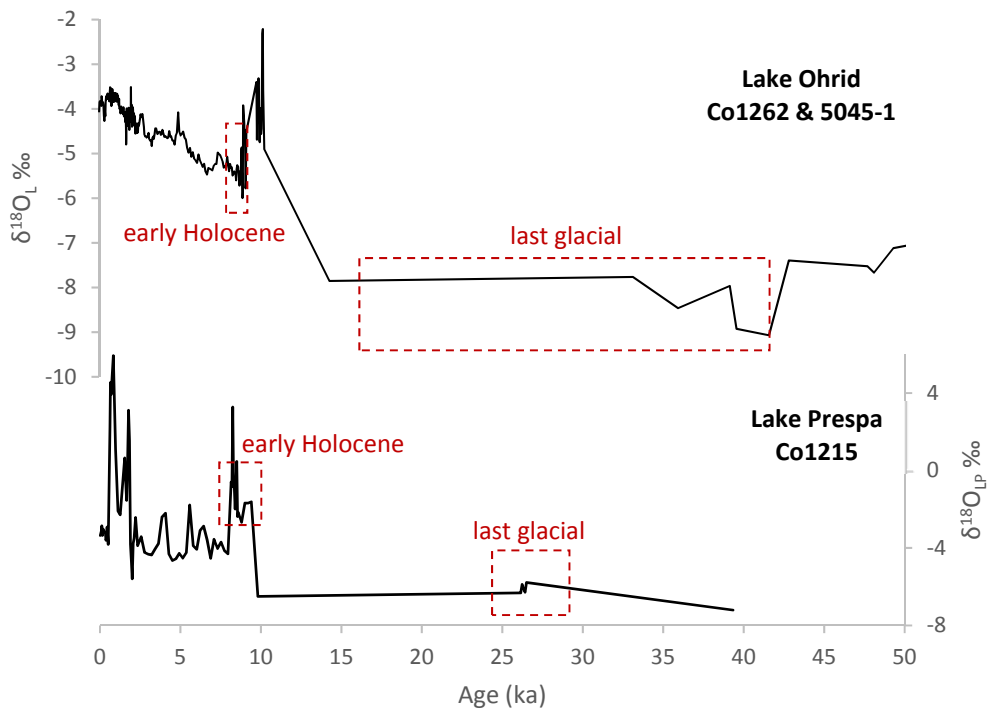
838 **Figure 3** Modern isotope composition ($\delta^{18}\text{O}$ and δD) of water from lakes Ohrid and Prespa,
839 springs, and local direct/catchment rainfall (Anovski et al., 1980; Anovski et al., 1991, 2001;
840 Eftimi and Zoto, 1997; Matzinger, 2006b; Jordanoska et al., 2010; Leng et al., 2010, 2013).
841 The global meteoric water line (GMWL; Craig, 1961), local meteoric water line (LMWL;
842 Anovski et al., 1991, Eftimi and Zoto, 1997), and calculated local evaporation line (LEL) are
843 shown.



844 **Figure 4** Iterative calculation of evaporation by using variable f and simultaneously evaluating
 845 hydrological and isotope mass balance equations to solve for G_iX and G_q (recent/Late
 846 Holocene), and P_L and Q_q (Early Holocene and last glacial), which are balanced for both $\delta^{18}O$
 847 and δD .

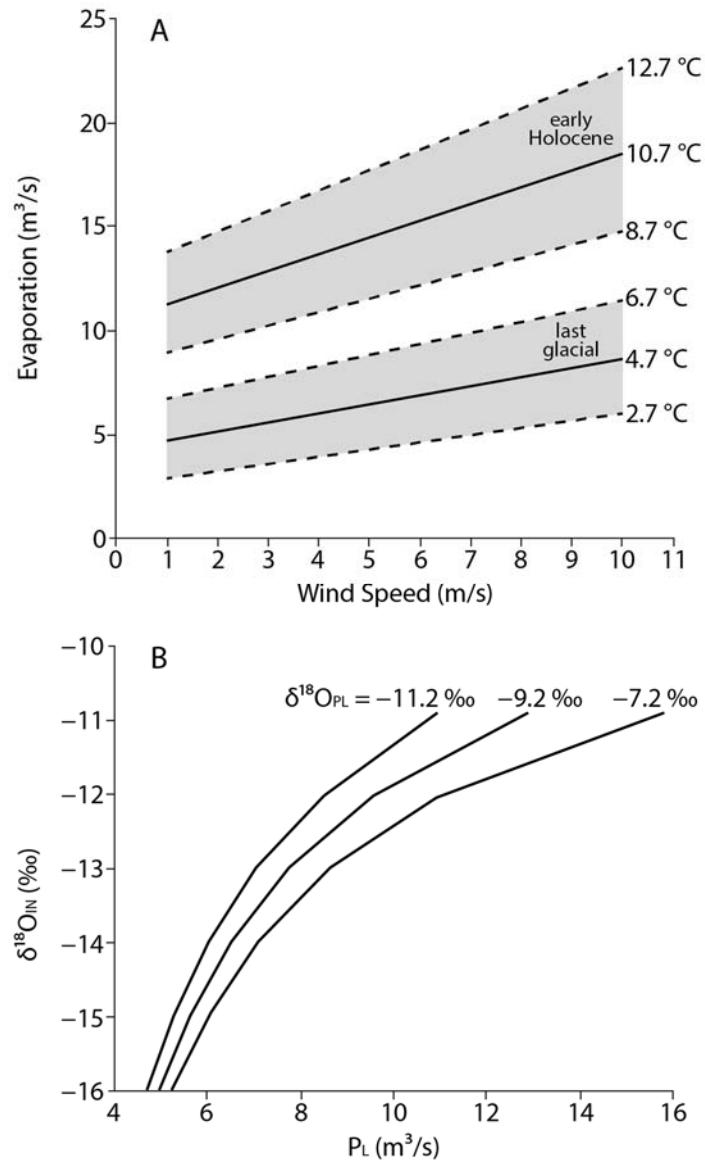


848 **Figure 5** Reconstructed oxygen isotope composition ($\delta^{18}\text{O}$) of lakewater from Lake Ohrid
849 cores Co1262 and 5045-1 (Lacey et al., 2015, 2016) and Lake Prespa core Co1215 (Leng et
850 al., 2013). $\delta^{18}\text{O}$ lakewater is calculated from calcite and siderite isotope data (see text for
851 calculation).



852 **Figure 6** Sensitivity of A) evaporation to changing wind speed at different temperatures for
853 the early Holocene and last glacial, and B) precipitation over the lake (P_L) to changing $\delta^{18}O_{IN}$
854 at different $\delta^{18}O_{PL}$ during the last glacial (all other parameters remain constant).

855



856 **Table 1** Relative proportions of meteoric precipitation and outflow from Lake Prespa
857 comprising spring inflow to Lake Ohrid.

Spring Complex	Component of Spring Inflow (m ³ /s)	
	Meteoric Precipitation	Lake Prespa Outflow
St. Naum	4.3 (58%)	3.2 (42%)
Tushemisht	1.2 (47%)	1.3 (53%)
Biljana	0.3 (100%)	0 (0%)
Total	5.8 (56%)	4.5 (44%)

858

859 **Table 2** Revised water balance for Lake Ohrid, including estimates for groundwater fluxes into
 860 and out of the lake. G_iX is the component of groundwater inflow sourced from meteoric
 861 precipitation, and G_Q is groundwater outflow.

Source	Flow rate (m³/s)
<u>Inputs</u>	
Precipitation (P_L)	8.8
Surface inflow (S_i)	7.2
Groundwater inflow (G_i)	
– Prespa-fed (G_iP)	7.7
– Surface springs (G_iS)	5.8
– Sublacustrine springs (G_iX)	G_iX
	29.5 + G_iX
<u>Outputs</u>	
Evaporation (E)	13.7
Surface outflow (S_q)	14.8
Groundwater outflow (G_q)	G_q
	28.5 + G_Q

862

863 **Table 3** New water balance for Lake Ohrid based on coupled hydrological and isotope mass
 864 balance modelling.

Source	Flow rate (m³/s)		δ¹⁸O (‰)	δD (‰)
<u>Inputs</u>				
Precipitation (P _L)	8.8	(20%)	-8.4	-52.9
Surface inflow (S _i)	7.2	(16%)	-10.1	-67.4
Groundwater inflow (G _i)				
- Prespa-fed (G _i P)	7.7	(17%)	-1.5	-20.5
- Surface springs (G _i S)	5.8	(13%)	-10.1	-67.4
- Sublacustrine springs (G _i X)	15.3	(34%)	-10.1	-67.4
<u>Outputs</u>				
Evaporation (E)	13.7	(31%)	-19.1	-112.7
Surface outflow (S _q)	14.8	(33%)	-3.5	-31.7
Groundwater outflow (G _q)	16.3	(36%)	-3.5	-31.7

865

866 **Table 4** Estimate of past hydrological balance of Lake Ohrid during the early Holocene and
 867 last glacial.

Source	Flow rate (m³/s)	δ¹⁸O (‰)	δD (‰)
Early Holocene			
<u>Inputs</u>			
Precipitation (P _L)	11.1	-8.7	-59.6
Inflow (I _i)	35.1	-10.4	-68.8
Prespa inflow (G _i P)	7.7	-2.1	-24.1
<u>Outputs</u>			
Evaporation (E)	12.3	-20.9	-125.3
Outflow (Q _q)	41.6	-5.3	-41.3
Last Glacial			
<u>Inputs</u>			
Precipitation (P _L)	4.9	-9.2	-62.3
Inflow (I _i)	15.4	-16.0	-98.9
Prespa inflow (G _i P)	7.7	-5.8	-44.0
<u>Outputs</u>			
Evaporation (E)	6.3	-25.5	-150.2
Outflow (Q _q)	21.7	-8.1	-56.4

868

869 **Table 5** Sensitivity of precipitation over the lake (P_L) to changing temperature during the early
 870 Holocene and last glacial. Evaporative flux varies with changing temperature, all other
 871 parameters remain constant.

Early Holocene					
T_{air} (°C)	T_{lake} (°C)	E (m ³ /s)	P_L (m ³ /s)	Q_q (m ³ /s)	f
8.7	11.0	9.8	9.2	36.3	0.35
10.7	13.0	12.3	11.1	41.6	0.36
12.7	15.0	15.1	13.1	47.2	0.36
Last glacial					
T_{air} (°C)	T_{lake} (°C)	E (m ³ /s)	P_L (m ³ /s)	Q_q (m ³ /s)	f
2.7	5.0	4.1	3.5	18.1	0.71
4.7	7.0	6.3	4.9	21.7	0.73
6.7	9.0	8.7	6.4	25.5	0.75

872